PHYSICOCHEMICAL PROPERTIES OF GLASS TESSERAE IN ROMAN TERRACE HOUSE FROM ANCIENT ANTANDROS (BASE GLASS, OPACIFIERS AND COLORANTS)

Zisan Kaplan*, Basak Ipekoglu and Hasan Boke

Department of Architectural Restoration, İzmir Institute of Technology

ABSTRACT

In this study, material characteristics of glass mosaic tesserae from Antandros ancient city, western Turkey, were investigated. The main objective of this study was to determine the compositional group of the glass tesserae. Their color, mineralogical, chemical and microstructural characteristics were determined using colorimeter, x-ray diffraction, x-ray fluorescence and scanning electron microscope. The results show that all the Antandros glasses were produced by using coastal sand as Levantine I glasses and exhibit similar compositions with natron type glasses (Roman type glasses), except for lower natron levels. Lower natron levels indicate that Antandros mosaic glass may have been produced in 7th century AD or natron may have been provided from a new flux source due to the shortage of Egyptian mineral soda or due to economic reasons glass manufacturers succeeded to produce same glass with low flux addition. Antandros glass tesserae were all opacified with antimony oxides and colored with transition metal oxides which are common used in Roman Period.

1.   INTRODUCTION

Glass was first produced in Mesopotamia around 2500 BC and was developed through to the Roman Period. In the Roman Period, a base glass batch consisted of sand as the source of silica and natron (soda) as flux. Silica and calcium carbonate containing sand was preferred and natron was used from the early-mid 1st millennium BC to the 9th century AD before the plant ash was used. It was obtained from the Wadi Natrun in Northern Egypt (Bimson and Freestone, 1988; Brill and Cahill, 1988; Lilyquist et al., 1993; Sayre and Smith, 1961). In the Roman Period glasses, had quite high Na_2O contents (16-20%). The drop-in soda contents start from the Late-Roman/Byzantine Period onwards. From the early Islamic Period, plant ash was used as alkaline flux in the glass batch instead of natron because of availability (Henderson, 1985). The glass was first produced in primary production centres, which were located near the sand and natron sources in Egypt (Sayre and Smith, 1961). The produced base glass was then distributed to secondary (local) glass workshops where additives (opacifiers and colorants) were introduced and glass was worked into a final product (Freestone et al., 2002).

During secondary production, glass was opacified using calcium or lead antimonate from about 1500 BC until antimony sources were depleted at the end of the Roman Period (Fiori et al., 2003). Opacification relies on two processes; addition of ex situ synthesized crystals to the raw glass or addition of raw compounds that lead to in situ crystallization of opacifying crystals in the glass melt (Lahlil et al., 2010b; Verita, 2000). Glass was colored by chromophore elements and opacifiers as coloring agent. Cobalt and copper oxides were used to obtain blue, green, purple and red colors in ancient glasses (Mirti et al., 2002; Newton and Davison, 1989). Iron oxide presented as natural traces in the sand however, it was also added intentionally to obtain different colors. Manganese oxide gives purple color to the glass and it was used as a de-colorant and combined with iron and cobalt to produce black and brown colors.

Throughout history, glass has been used as beads, bottles, vessels, windowpanes, and mosaic tesserae. Most of the studies concerning ancient glass compositions are about glasses that were originated from Hellenistic to Late Byzantine Period and they reported the origin and production technologies of glass and its raw materials, colorants and opacifiers (Arletti et al., 2006b; Brill, 1968; Fiori, 2015; Freestone, 1987; Henderson, 1988; Möncke et al., 2014; Rehren and Freestone, 2015; Sayre and Smith, 1961; Schibille, 2011; Shortland and Tite, 2000; Silvestri et al., 2011; Turner, 1956). In Turkey, there are few studies concerning glass compositions. Brill (1999), investigated early glass compositions and prepared a catalogue including glass compositions from Sardis in western Anatolia and Aphrodisias in southwestern Anatolia. Uhlir et al., (2006), investigated compositions of glass objects from the Late Hellenistic to Late Byzantine period at Terrace House I, Ephesus in western Anatolia. Schibille, (2011), provided chemical and technological data of Byzantine glass production, and collected chemical data from Pergamon in northwestern Anatolia. Schibille et al., (2012), also determined the origin, and production technology of Byzantine glass tesserae from Sagalasos, in southwestern Anatolia. Rehren et al., (2015), reports compositional data of Roman glass from Pergamon Turkey.

In addition, Lauwers et al., (2007) studied local glass workshops in Anatolia. They determined the local glass workshops that built during the late Roman and Byzantine Periods in Turkey according to previous studies (Figure 1).

Although there are only a few studies concerning glass compositions in Turkey, there is still a lack of analytical data concerning the production technology and compositions of mosaic glass tesserae from Anatolia. This study presents the chemical data of glass tesserae found during excavations of Antandros Ancient City, Turkey. The aim of the study is to determine the compositional groups of the mosaic glass to contribute to the analytical data of the ancient glasses found in Turkey.

2.   ARCHEOLOGICAL BACKGROUND

Antandros was located on the top and western slopes of Dervent Hill (Kaletaşı Hill), at an altitude of 215 m, descending steeply down to Adramyttion (Edremit) Gulf in western Turkey (Figure 1). Antandros was an imported city of the ancient Torad Region, it was a harbour city and famous for its dockyards. Strabo, 2000, mentions a harbour in Antandros, called Aspaneus where timber was exported. The city dates back from late 6th century BC to Byzantine Period. After Arab invasions in 6th century AD, a new settlement was established in Antandros and the city became a Bishopric Centre (Quien M. Le, 1958). It was completely abandoned in 14th century. In 1989, the area was zoned for housing and graves (Necropolis) were found and salvage excavations were started in 1991 (Yalman, 1993). In 2001, archaeological excavations started and a Roman Terrace House, with its bath complex was found.

Figure 1. Late Roman and Byzantine Periods secondary glass production sites in Anatolia and Location of Antandros

Terrace House was built in early 4th century AD and it was used until the 6th -7th centuries AD. The House was similar to Roman Terraced House typology due to its rows of spaces on one side of the portico (Smith, 1997). The house was oriented from east to west. It has a rectangular plan and an adjacent bath complex at the south east of the house (Figure 2). There were a portico and a *kriptoportico* (upper portico). The portico was located on the sea side of the house with 32.90×4.30 m dimensions and its floor was covered with well-preserved mosaics. There were six rooms at the north and a *latrine* (toilet) to the east of the portico. Two of the six adjacent rooms were *triclinia* used in summer and winter (welcoming spaces) and one room decorated with well-preserved floor mosaics (Figure 1).

Figure 2. Plan of the Terrace House and the spaces covered with mosaics
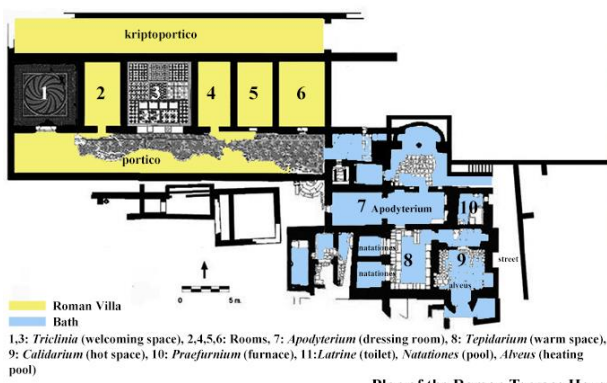
On the south-east corner of the portico there is a stair reaching to the bath with circular steps. Spatial characteristics of the bath were altered due to usage changes and deformations in the past (Polat et al., 2007). *Apodyterium* (dressing room-space 7) is situated at the west of the bath, it has a rectangular form with 11.63×3.40 m dimensions. Floor of the *apodyterium* is covered with mosaics and the on walls there

are remains of wall paintings (Figure 2). *Tepidarium* (warm space-space 8), is situated at the south of *apodyterium,* it has rectangular form with 6.20×4.15 m dimensions. There is an opening between *apodyterium* and *tepidarium* to provide connection. Mortar traces of *sectile* mosaics are observed on the floor of *tepidarium*. Two *natationes* (pool) situated at the west of the *tepidarium* and they are in square form with

2×2.30 m. *Calidarium* (hot space-space 9) is situated at the east of the *apodyterium,* it has rectangular form with 3.5×4.15 m dimensions. At the south of the *calidarium* there is an *alveus* (hot water pool). Floor of the *calidarium* was elevated due to the renewing of the hypocaust system. *Praefurnium* (furnace-space 10) of the bath is situated north of the *calidarium,* it has a square form with 1.95×2.90 m dimensions which was converted into a furnace. There is another space (space 11) situated at the north of the *apodyterium*, it has rectangular form with 5.30 m width (Polat, 2002; Polat et al., 2007; Polat and Polat, 2005).

In Roman times, the size of the house, style, decoration of the house was related with the social class of the owner. The most important rooms were decorated with mosaic pavements. Mosaic patterns were designed according to the function of the space. Mosaic pavements give clues to the date, technique, craftsmen, and the use of the room and the function of the house.

3.   MATERIALS AND METHODS

In this study, eighteen opaque colored glass tesserae were chosen from broken mosaics of the *portico* and *kriptoportico* of the terrace house. Samples were labelled with the first one or two letters of their colors. (Table 1). The tesserae contain yellow, green, cyan, turquoise, blue, light brown, dark red, black and white colors. All tesserae are opaque except one semi-opaque blue and one semi-opaque white tesserae. They were all preserved with minor surface pitting and corrosion. All the analysis was carried out after weathering layers were removed and samples were washed with distilled water and dried at 60°C in an oven. Color measurements were done with washed samples. For the X-Ray Fluorescence (XRF) and X-ray Diffraction analysis (XRD), small fragments were taken from each tesserae and ground into fine powder. For Scanning Electron Microscope Analysis (SEM), small sections were cut and left uncoated.

Table 1. Glass tesserae samples

Name	Transparency	Photo	Name	Transparency	Photo	Name	Transparency	Photo
Y	Opaque		**T1**	Opaque		**Bv-O**	Opaque	
Lg	Opaque		**T2**	Opaque		**Bv-So**	Semi-Opaque	
Dg1	Opaque		**Dt**	Opaque		**Lbr**	Opaque	
Dg2	Opaque		**C1**	Opaque		**W**	Semi-Opaque	
G1	Opaque		**C2**	Opaque		**Dr**	Opaque	
G2	Opaque		**Lb**	Opaque		**B**	Opaque	
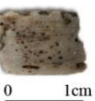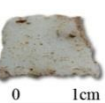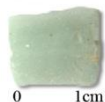
In the experimental stage of this study, colors of the tesserae were identified by using a colorimetric measurement instrument (Avantes) by Avasoft 6.2. Measurements were conducted on homogenous flat and smooth surface with 4mm diameter spot size, D65 daylight illuminant and 10° observer. Results are expressed by colorimetric coordinates (L, a, b, C, h, X, Y, Z) in the CIEL *a*b color space system based on Commission Internationale de I' Eclairage colors. The L*, a* and b* values were converted into RGB values with an online "Color Calculator" program (www.easyrgb.com) and expressed on the coordinate system with CIELab (L*a*b) color sphere using Microsoft Office Excel 2012 and Adobe Photoshop CS4 software. In this color system L* is the lightness factor (L*=0 black; L*=100 white), a* is the value between green and red (-a*= green; +a*=red), and b* is the value between blue and yellow (-b*=blue; +b*=yellow) (CIE).

Major and minor elements of tesserae were identified by XRF (Ali and Abd-allah, 2015; Arinat et al., 2014). Analysis were carried out on powdered samples using a Spectro IQ-II on melt tablets with 0.01% detection limit. Powdered samples were dried at 105°C and calcinated at 1000°C, then they were diluted with lithium tetra borate by Materials Research Center in Izmir Institute of Technology.

X-Ray diffraction analysis were performed on powdered samples to determine the crystalline phases with Philips X-Pert Pro X-Ray Diffactrometer. The spectra were collected at 40 kV and 40mA from 5° to 60° with 2θ and processed by using Philips X-Pert Pro Software.

Microstructural characteristics of glass tesserae were determined using Philips XL 30S FEG scanning Electron Microscope (SEM) equipped with X-Ray Energy Dispersive System (EDS) located at the Izmir Institute of Technology Center for Materials Research, Turkey. Backscattered images (BSE) were taken at 15-20 kV accelerating voltage with a beam size from 2μm to 500μm.

In general, mosaic glass tesserae show compositional homogeneity, such as bands or mineral inclusions besides the opacifiers and colorants. For this reason, analysis was carried out on both SEM-EDS to match the micro texture with the chemical composition. For more precise elemental compositional data XRF analysis were carried out. In addition, to identify the crystal shape of opacifiers SEM-EDS analysis were done.

4. RESULTS AND DISCUSSION

Surface colour properties of the glass tesserae were determined and expressed using colorimetric coordinates (L*, a*, b*, C*, h, X, Y, Z) in the CIEL*a*b* colour space system. Colours were determined, to the high and low positions of positive and negative values of *a and b* values of CIEL*a*b* colour space system, as black, red, brown, yellow, green, blue, cyan, turquoise, white and their shades (Figure 3).
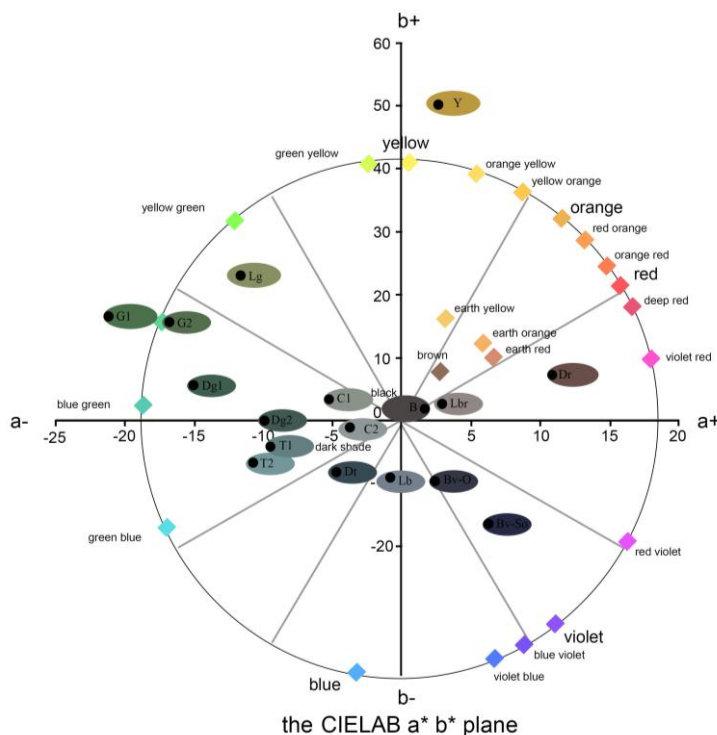
*Figure 3. Colours of the samples in CIELa*b* color space*

Only the green, blue and turquoise glasses have different shades of color. Green glasses are two green, light green and two dark green. Blue glasses are one light blue and two dark blue. Turquoise glasses are one light turquoise, one turquoise and one dark turquoise. The L*, a*, b*, C and h values and coloring agents of the tesserae are given in Table 2.

High positive b*values and low positive a* values correspond to yellow glass containing high lead and low antimony contents. Green samples have variable positive b* values and low negative a* values that are distinguished by both high lead and high copper contents. A significant number of tesserae have variable negative b* and a* values that have high antimony and low lead contents these are cyan, turquoise and blue samples. Dark red sample has distinctive high positive a* and b* values that are distinguished with high iron content. Brown and black samples have weak positive b* and a* values ~1, whereas brown contains high antimony and black contains high Fe_2O_3 (

Table 2).

Table 2. Colorimetric coordinates, opacifiers and colorants of the glass tesserae.

Name-Colour	Colorimetric Coordinates					Elements							Opacifier	Colorant
	L	a	b	C	h	Sb_2O_5	ZnO	CoO	MnO	CuO	PbO	Fe_2O_3		
Y Yellow	64.73	2.6	50.21	50.28	87.03	1.02%	0.03%	0.01%	0.40%	0.49%	19.3%	0.85%		PbO
Lg Light Green	57.95	-11.69	23.03	25.83	116.92	0.83%	0.03%	0.01%	0.42%	0.88%	22.6%	1.02%	Pb-antimony ($Pb_2Sb_2O_7$)	PbO+CuO
Dg1 Dark Green	37.03	-15.01	5.63	16.04	159.43	0.64%	0.38%	0.01%	0.73%	2.65%	6.61%	0.80%		
Dg2 Dark Green	35.49	-9.95	0.06	9.95	179.65	0.58%	0.04%	_	0.46%	1.80%	16.2%	0.71%		
G1 Green	43.57	-21.19	16.54	26.88	142.03	0.86%	0.03%	0.01%	0.50%	2.39%	18.9%	0.85%		
G2 Green	43.73	-16.81	15.71	10.59	136.93	0.77%	0.03%	_	0.48%	1.70%	17.4%	0.82%		
T1 Turquoise	51.13	-9.5	-4.18	10.38	203.77	3.46%	0.03%	_	0.50%	3.25%	0.06%	0.69%	Ca-antimony ($CaSb_2O_6$)	CuO+CoO
T2 Turquoise	60.12	-10.77	-6.69	12.68	211.86	3.44%	0.02%	_	0.39%	0.74%	0.09%	0.49%		
Dt Dark Turquoise	29.76	-4.79	-8.26	9.55	239.91	1.41%	0.02%	_	0.49%	2.56%	0.13%	0.57%		
C1 Cyan	59.89	-5.32	3.34	6.28	147.92	4.07%	0.01%	_	0.49%	0.35%	0.29%	0.79%		CoO
C2 Cyan	62.45	-3.74	-1.1	3.9	196.47	4.22%	_	0.01%	0.50%	0.30%	0.35%	0.75%		
Lb Light Blue	54.16	-0.81	-1.71	1.89	244.57	3.26%	_	0.02%	0.46%	0.07%	0.27%	0.59%		
Bv-O Dark Blue	23.47	2.36	-9.68	9.96	283.72	4.27%	_	0.11%	0.36%	0.16%	0.18%	1.11%		
Bv-So Dark Blue	17.64	6.21	-16.46	17.59	290.66	2.03%	_	0.07%	0.41%	0.10%	0.04%	0.85%		
Lbr Light Brown	57.34	2.9	2.72	3.98	43.2	3.10%	_	_	2.38%	0.04%	0.05%	0.54%		MnO
W White	80.21	1.69	8.25	8.42	78.46	1.68%	0.01%	_	0.07%	0.02%	0.19	0.44%		Ca-antimony
B Black	30.32	1.64	1.87	2.48	48.84	_	_	_	0.05%	_	_	5.61%	--	Fe_2O_3
Dr Dark Red	35.77	10.81	7.18	12.97	33.6	0.59%	0.02%	_	0.65%	1.07%	2.00%	3.81%	Iron oxides, copper oxides	$CuO.Fe_2O_3$

Table 3. Major elements of glass tesserae by XRF in wt % of the oxides

Sample[1] Elements	Y	Lg	Dg1	Dg2	G1	G2	T1	T2	Dt	C1	C2	Lb	Bv-O	Bv-SO	Lbr	W	B	Dr
SiO_2	59.18±0.07	56.05±0.07	66.27±0.08	60.78±0.07	58.37±0.07	59.29±0.07	69.08±0.08	71.95±0.08	71.57±0.08	69.99±0.08	70.22±0.05	72.05±0.08	69.78±0.08	72.51±0.08	69.90±0.08	76.21±0.08	65.96±0.05	68.55±0.08
Na_2O	6.27±0.08	5.90±0.08	6.70±0.073	6.25±0.076	5.67±0.075	6.18±0.077	6.83±0.07	7.75±0.074	7.49±0.072	7.39±0.073	7.61±0.074	8.08±0.075	6.98±0.07	8.50±0.075	7.66±0.075	8.35±0.075	10.51±0.08	7.07±0.073
CaO	6.81±0.027	6.73±0.028	9.17±0.027	7.38±0.027	6.69±0.027	7.51±0.028	8.76±0.026	7.96±0.025	8.92±0.025	8.22±0.028	7.97±0.028	7.61±0.026	9.59±0.027	8.64±0.025	9.05±0.026	6.92±0.022	7.39±0.015	9.06±0.025
Al_2O_3	2.31±0.016	2.14±0.016	2.57±0.015	2.26±0.015	2.21±0.015	2.30±0.016	2.56±0.015	2.41±0.014	2.50±0.015	2.76±0.015	2.49±0.015	2.38±0.014	2.77±0.015	2.45±0.014	2.51±0.014	2.14±0.014	3.13±0.016	2.81±0.015
MgO	0.99±0.017	0.98±0.018	1.11±0.016	1.01±0.017	0.94±0.017	0.99±0.017	1.12±0.015	1.15±0.015	1.15±0.015	1.25±0.015	1.19±0.015	1.17±0.015	1.17±0.015	1.17±0.014	1.18±0.015	1.13±0.014	2.22±0.027	1.20±0.015
K_2O	0.33±0.013	0.26±0.014	0.57±0.011	0.37±0.013	0.30±0.013	0.35±0.013	0.62±0.01	0.56±0.01	0.59±0.01	0.62±0.011	0.57±0.011	0.84±0.0092	0.51±0.0099	0.69±0.011	0.67±0.01	0.43±0.0099	0.49±0.0078	0.64±0.011
P_2O_5	0.48±0.0061	0.51±0.0064	0.34±0.0046	0.42±0.0055	0.46±0.058	0.43±0.0057	0.23±0.0039	0.23±0.0039	0.23±0.0039	0.27±0.004	0.26±0.004	0.25±0.0039	0.23±0.0038	0.24±0.0039	0.28±0.0039	0.17±0.0038	0.16±0.0018	0.31±0.004
SO_3	–	–	0.28±0.0087	–	–	–	0.98±0.0037	0.97±0.0036	0.47±0.0027	1.22±0.004	1.17±0.004	0.92±0.0039	1.05±0.004	0.65±0.003	0.75±0.0032	0.50±0.0027	0.23±0.0009	0.37±0.0048
Cl	0.69±0.002	0.65±0.0021	0.85±0.0017	0.75±0.0019	0.64±0.019	0.77±0.002	0.98±0.0017	1.03±0.002	1.09±0.002	0.99±0.0017	0.98±0.0017	1.04±0.002	0.74±0.0014	0.95±0.0017	0.99±0.0017	1.11±0.002	0.55±0.0011	0.97±0.0017
TiO_2	0.10±0.0044	0.11±0.0044	0.12±0.0037	0.12±0.0041	0.11±0.042	0.13±0.0042	0.14±0.0041	0.12±0.004	0.12±0.0039	0.13±0.0043	0.11±0.0042	0.09±0.0042	0.12±0.0039	0.14±0.0039	0.12±0.0041	0.12±0.0039	0.08±0.0017	0.14±0.0037
MnO	0.40±0.0073	0.42±0.0078	0.73±0.0069	0.46±0.0069	0.50±0.072	0.48±0.0077	0.50±0.0059	0.39±0.0053	0.49±0.0058	0.49±0.0061	0.50±0.006	0.46±0.0055	0.36±0.0053	0.41±0.0051	2.38±0.011	0.07±0.0038	0.05±0.0029	0.65±0.0069
Fe_2O_3	0.85±0.0065	1.02±0.007	0.80±0.0057	0.71±0.0058	0.85±0.0065	0.82±0.0064	0.69±0.0052	0.49±0.0042	0.57±0.0047	0.79±0.0055	0.75±0.0053	0.59±0.0046	1.11±0.006	0.85±0.0053	0.54±0.0053	0.44±0.0038	5.61±0.009	3.81±0.012
SrO	0.12±0.0018	0.08±0.002	0.07±0.001	0.13±0.0016	0.07±0.0017	0.10±0.0017	0.08±0.00066	0.09±0.00063	0.09±0.00073	0.11±0.00064	0.12±0.00067	0.12±0.00065	0.07±0.00063	0.12±0.00059	0.08±0.0007	0.05±0.00062	0.05±0.00033	0.10±0.0012
CuO	0.49±0.0041	0.88±0.0054	2.65±0.007	1.80±0.007	2.39±0.008	1.70±0.006	3.25±0.007	0.74±0.0033	2.56±0.006	0.35±0.0028	0.30±0.0026	0.07±0.0019	0.16±0.0021	0.10±0.0018	0.04±0.0017	0.02±0.0014	–	1.07±0.005
SnO_2	0.08±0.0038	0.12±0.0049	0.04±0.0019	0.20±0.0045	0.20±0.0049	0.12±0.0042	0.39±0.0035	0.09±0.0025	0.44±0.0048	0.07±0.0018	0.07±0.002	0.03±0.0013	0.02±0.00098	–	0.02±0.0012	–	–	0.10±0.0044
Sb_2O_5	1.02±0.006	0.83±0.0056	0.64±0.0046	0.58±0.0042	0.86±0.0051	0.77±0.0049	3.46±0.008	3.44±0.009	1.41±0.006	4.07±0.008	4.22±0.009	3.26±0.008	4.27±0.009	2.03±0.007	3.10±0.008	1.68±0.006	–	0.59±0.0085
Ta_2O_5	0.47±0.013	0.50±0.018	–	0.44±0.021	–	0.46±0.021	–	0.23±0.011	–	–	0.45±0.0085	0.43±0.0057	0.35±0.0066	0.36±0.0056	0.33±0.0049	0.30±0.0043	–	–
CoO	0.01±0.0018	0.01±0.0019	0.01±0.001	–	0.01±0.0013	–	–	0.02±0.0021	0.00326±0.00079	–	0.01±0.0011	0.02±0.0014	0.11±0.0023	0.07±0.0019	–	–	–	–
PbO	19.31±0.03	22.66±0.03	6.61±0.013	16.27±0.03	18.95±0.03	17.48±0.03	0.06±0.0019	0.09±0.014	0.13±0.0017	0.29±0.0038	0.35±0.004	0.27±0.0021	0.18±0.0021	0.04±0.0011	0.05±0.0011	0.19±0.0018	–	2.00±0.007
Total[2]	99.90%	99.90%	99.55%	99.93%	99.25%	99.92%	99.73%	99.66%	99.81%	98.96%	99.29%	99.62%	99.56%	99.88%	99.67%	99.84%	96.41%	99.41%

[1] Sample: Sample names as the first one or two letter of their colours, [2] Other Oxides: Ba, Te, Mo, V_2O_5, I, Br, Nb_2O_5,

4.1. Base Glass

Elemental composition of each sample was identified with XRF analysis. Results show that glass tesserae are soda lime silica and lead glasses composed of SiO_2 (56.05%-76.21%), Na_2O (5.67%-10.51%) and CaO (6.69%-9.59%) (Table 3). Lead glasses contain higher amounts of PbO (n.d-22.66%) in yellow and green samples, which is a peculiar glass characteristic, responsible for the strong colours and lower melting point of the glass batch (Vandini et al., 2006).

Analysed tesserae from Antandros show low MgO (0.94%-1.25%) and low K_2O (0.26%-0.84%) (Figure 4) which indicates that the glass tesserae are natron type glass (Brill, 1999). Another fact that indicates the use of natron is the considerable amounts of Cl (0.55%-1.11%) and SO_3 (0.23%-1.22%) which exist as deposits in sodium carbonates (Silvestri et al., 2012b). Furthermore lower (< 0.15%) P_2O_5 contents (0.16%-0.51%) also indicate the use of natron (Sayre and Smith, 1961).
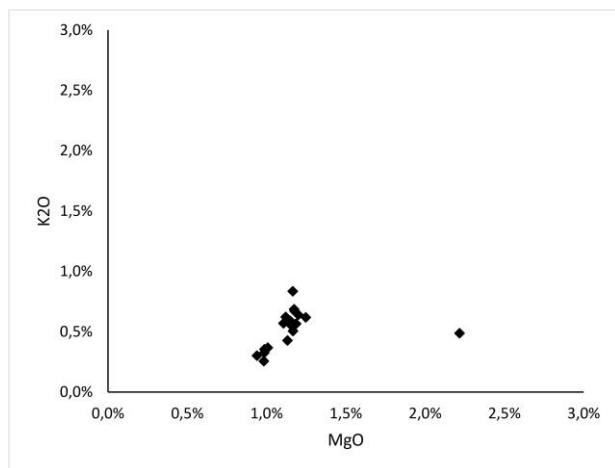
Figure 4. K₂O% versus MgO% diagram of glass tesserae.

Based on magnesium and potassium levels, of analysed Antandros tesserae are natron based glasses, however, the detected Na_2O levels are lower than natron glasses as determined in literature (12-20%) (Table 4) except black tesserae (B) (10.51%).

Therefore, a comparison with similar studies related with glass tesserae was done to clarify the glass production period and the compositional group. In Table 4 concentrations of SiO_2, Na_2O, CaO, Al_2O_3, MgO, K_2O and MnO were compared since they are diagnostic for compositional groups. In Table 4, analysed glasses show similar concentrations with previous studies except for Na_2O. In addition, analysed tesserae were compared with Roman blue-green glasses by Jackson et al., 1991 and glass groups identified by Freestone, 2006, from Levant to Egypt between 4th to 8th centuries (Table 5). They are all natron based glasses and exhibit different major and minor oxides due to impurities in the sand and flux. Also, glasses were compared with Early Islamic plant ash glasses (Freestone et al., 2002; Gratuze and Barrandon, 1990; Silvestri et al., 2012b; Tite et al., 2007).

Another comparison was made with Byzantine mosaic glass that was identified by Vandini et al., 2006 and Arinat et al., 2014. The analyzed tesserae exhibit similar compositions to that Late Byzantine glass from Dafni in Greece, in Late Byzantine, 11th century A.D and 6th to 7th century A.D glass mosaic tesserae from the Cross church in Jerash in northern Jordan which contains lower levels of natron (5-13%).

In comparison, it is shown that glass tesserae exhibit similar compositions with natron type glasses (Roman type glasses), except for lower natron levels. It can be suggested that Antandros mosaic glass may have been produced in 7th century AD. Another suggestion is that, natron may have been provided from a new flux source due to the shortage of Egyptian mineral soda or due to economic reasons glass manufacturers succeeded to produce same glass with low flux addition.

In literature, Pergamon (4th-14th century AD) and Aphrodisias (5th -7th century AD) glasses contained different alkali and alkali earth materials such as boron, lithium and strontium which indicates a different flux source in western Anatolia surrounding Pergamon (Brill, 1988; Schibille, 2011). Another comparison was made on CaO and Al_2O_3 contents as they reflect the silica source. CaO (6.81% to 9.59%) and Al_2O_3 (2.14% to 3.13%) contents are compared in Figure 5 with reference data obtained by Freestone with Wadi Natrun, Egytp II, Bet Eli'ezer, Levantine I and HIMT glasses from Mediterranean Area (4th -9th A.D) to evaluate the possible origin of the glass. According to Figure 5, the sand used in the manufacture of Antandros glasses show similar concentrations with Levantine I glass (Freestone, 2005). However, black tesserae show different characteristics from Levantine I group glasses.
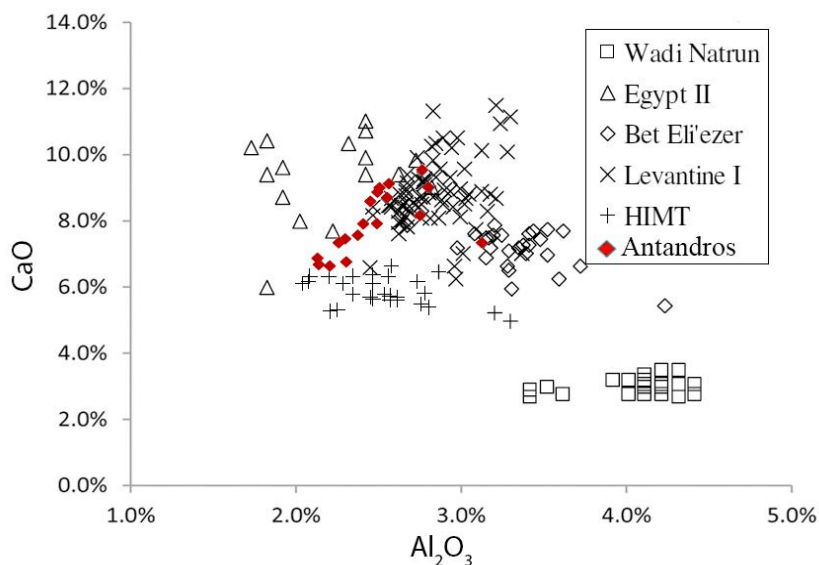
Figure 5. CaO% versus Al₂O₃% diagram of glass tesserae. Source: (data except Antandros from Freestone, 2005)

Besides alumina, iron oxides and titanium oxides are important to define the different sand sources. In Figure 6, Fe_2O_3 versus Al_2O_3 graph, data are compared with five glass groups (Freestone et al., 2002) and Antandros glasses show similarities with Levantine I group. In this graph, black and red tesserae are similar with the high iron magnesia titanium (HIMT) group glasses due to their higher iron contents.
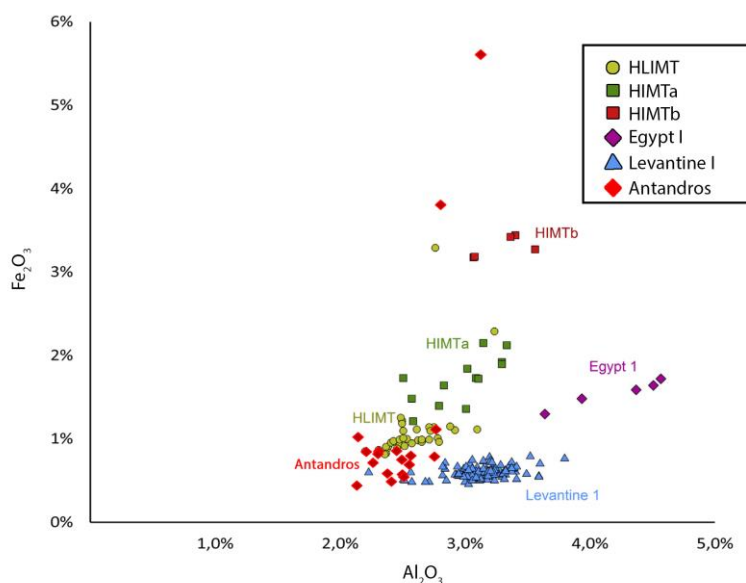
Figure 6. Fe₂O₃ % versus Al₂O₃% diagram of glass tesserae. Source: (data except Antandros from Ceglia et al., 2015)

The TiO_2 levels (0.08%-0.14%) indicate that glasses were produced by the same silica sources. When analyzed tesserae were compared with TiO_2 levels of Levantine glasses, it can be suggested that glasses were produced with the sand from Levantine coast due to their low TiO_2 levels (Foy, 2000; Freestone et al., 2015).

Strontium levels also indicate the source of the sand as either coastal or inland sands. Strontium concentrations are derived from the shell fragments in the sand (Freestone, 2005; Freestone et al., 2003; Silvestri et al., 2008; Wedepohl and Baumann, 2000; Werf et al., 2009). Analyzed tesserae have high amounts of SrO (0.05%-0.13%) that indicates the use of coastal sand in the glass manufacture except for black tesserae.

These results suggest that all the Antandros glasses were produced by using coastal sand as Levantine I glasses (Freestone, 2005) except black tesserae. Black tesserae may have been produced with a different sand and natron source.

Table 4. Comparison of chemical compositions of glasses with similar studies

	Glass tesserae										Glass	
	XRF	SEM/EDS	EPMA	EMPA	WDS-EPMA	SEM/EDS	ICP-MS	EPMA	EDS-WDS	ICP	EPMA	EPMA
	2017	(Paynter et al., 2015)	(Schibille et al., 2012)	(Silvestri et al., 2011)	(Arletti et al., 2011a)	(Croveri et al., 2010)	(Werf et al., 2009)	(Arletti et al., 2006b)	(Mass J. L et al., 2002)	(Costagliola et al., 2000)	(Schibille, 2011)	(Rehren et al., 2015)
	Antandros 4th AD	West Clacton, 2nd AD	Sagalassos 6th AD	Padova Italy (6th AD)	Florence Baptistery 4th -5th AD	Enna Italy, 3rd -4th AD	Herculaneum Italy 1st AD	Pompeii	Amorium	Florence Italy	Pergamon	Pergamon
SiO$_2$	56.05-76.21	53.69-69.30	45.02-71.23	63.8-70.4	40.07-64.21	58.66-68.35	55.00-68.07	46.35-98.65	52.8-69.4	43.38-98.25	65.85-73.49	65.0-73.1
Na$_2$O	**5.67-10.51**	**13.30-19.13**	**12-20.55**	**13.3-18.7**	**1.78-14.39**	**16.65-20.76**	**7.95-19.76**	**0.08-18.23**	**13.0-19.2**	**nd-18.00**	**14.51-18.57**	**14.8-18.9**
CaO	6.69-9.59	4.80-7.68	4.45-7.83	5.2-9.1	4.42-10.60	4.82-7.44	2.82-10.97	0.02-14.30	6.6-10.7	0.07-18.30	6.24-9.10	5.3-8.6
Al$_2$O$_3$	2.14-3.31	1.82-2.58	1.64-3.28	1.79-2.51	0.55-2.84	0.92-2.17	1.05-3.04	0.01-2.81	2.1-3.0	0.45-4.77	1.78-3.13	1.68-2.59
MgO	0.94-2.22	0.34-2.79	0.42-1.42	0.41-1.28	0.74-4.24	0.74-2.56	0.25-2.12	0.01-1.01	0.5-2.7	0.14-3.23	0.38-0.95	0.32-0.68
K$_2$O	0.26-0.84	0.54-2.11	0.28-1.71	0.39-0.79	0.68-25.37	0.61-1.50	0.49-4.13	nd-0.9	0.5-1.6	nd-5.05	0.44-0.78	0.37-1.11
FeO	0.44-5.61	0.52-1.69	0.40-7.67	0.31-1.25	0.24-2.05	0.47-2.10	0.53-3.01	nd-0.92	0.38-5.4	0.17-2.39	0.29-2.85	0.22-1.39
MnO	0.05-2.38	<0.1-0.93	0.04-1.75	<0.05-2.00	0.05-2.6	nd-1.05	0.07-1.22	nd-5.44	0.03-2.6	nd-2.65	nd-3.66	nd-1.43

EMPA: Electron microprobe analysis

Table 5. Comparison of Antandros glasses with glass composition groups

		Roman	Late Roman	Byzantine	Early Islamic	Early Islamic
		Blue-green	**HIMT**	**Levantine I**	**Levantine II**	**Plant ash**
	Antandros	(Jackson et al., 1991)	(Freestone et al., 2002)	(Freestone and Gorin-Rosen, 1999)	(Freestone, 2000)	**Freestone&Leslie (unpublished)**
	4th AD	1-3rd A. D	4-5th A. D	6-7th A. D	7-8th A. D	10-13th A. D
SiO$_2$	56.05-76.21	na	65.80	69.30	74.90	70.50
Na$_2$O	**5.67-10.51**	**18.40**	**18.00**	**15.60**	**12.10**	**12.50**
CaO	6.69-9.59	6.43	5.99	9.17	7.16	8.55
Al$_2$O$_3$	2.14-3.31	2.33	2,69	3.03	3.32	1.06
MgO	0.94-2.22	0.55	0.94	0.59	0.63	2.72
K$_2$O	0.26-0.84	0.69	0.46	0.63	0,46	1.89
MnO	0.05-2.38	0.26	1.51	<0.1	<0.1	1.00
FeO	0.44-5.61	0.6	2.18	0.45	0.52	0.40

Source: Freestone and Hughes, 2006

4.2. Opacifiers and Colorants

Opacifiers of the glasses were determined by XRD analysis. Shapes, sizes and distribution of the opacifiers were determined by SEM analysis. Abundance of crystals were calculated using XRF results. Antimony based opacifiers were detected.

Considerable amounts of antimony in glass compositions (0.59-4.27 %) were determined, except black sample. The XRD analysis and BSE images confirmed that small crystals were dispersed in the glassy matrix with different shapes and sizes.

Lead antimonate crystals (yellow-$Pb_2Sb_2O_7$) were identified in yellow and green tesserae (Figure 7). They are both densely and homogenously dispersed in yellow and green glass.

The amount of $Pb_2Sb_2O_7$ crystals dispersed in the matrix is approximately 1.38% to 2.43%. The size of crystals varies between 0.3 µm-1.2 µm. Lead antimony was determined with euhedral and tiny acicular in yellow and tiny acicular shapes in green samples as they were produced by ex situ crystallization (Figure 8). Similar observations had been obtained by Lahlil et al., 2008; Schibille et al., 2012; Silvestri et al., 2012b.
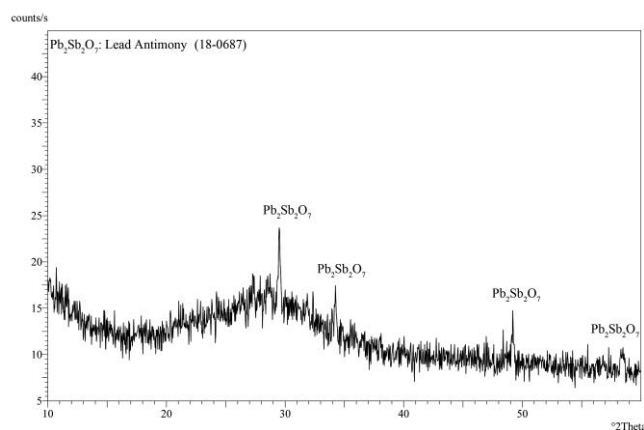
Figure 7. XRD pattern of yellow tesserae
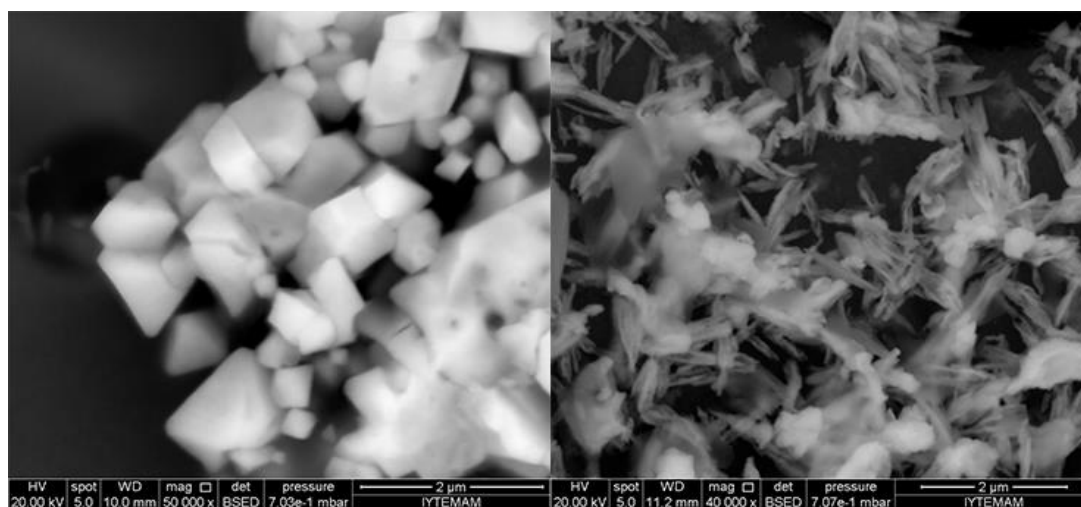
Figure 8. BSE images of Pb antimonate crystals as hexagonal in yellow (left) and tiny acicular in green (right)

Calcium antimonate crystal (white-$CaSb_2O_6$) were identified in turquoise, blue, cyan, white and brown tesserae. The BSE images of blue, turquoise, dark turquoise, and cyan samples shows different density of Ca antimony crystals than semi opaque white and blue samples. They are densely and homogenously well dispersed in the glassy matrix. They have euhedral (hexagonal) shapes which indicates that the glass was opacified with in situ crystallization by adding roasted stibnite to the glass melt (Figure 9) (Schibille et al., 2012).

Total amount of dispersed crystals in the matrix is approximately 3.64% to 4.95%. The size of crystals varies between 0.1 µm- 1 µm. In the XRD analysis, $CaSb_2O_6$ diffraction patterns confirm the crystals in BSE images (Figure 10).

In BSE images of semi-opaque white tesserae, a few Ca-antimony crystals were determined dispersed in the matrix which is less than the other tesserae. In semi, opaque blue tesserae, the glassy matrix contains a few Ca antimony crystals similar with the white glass. The number of particles per unit

volume indicates different opacity degrees in Ca antimony glasses. Therefore, it can be suggested that

Pb antimony is a more effective opacifier than the Ca antimony.
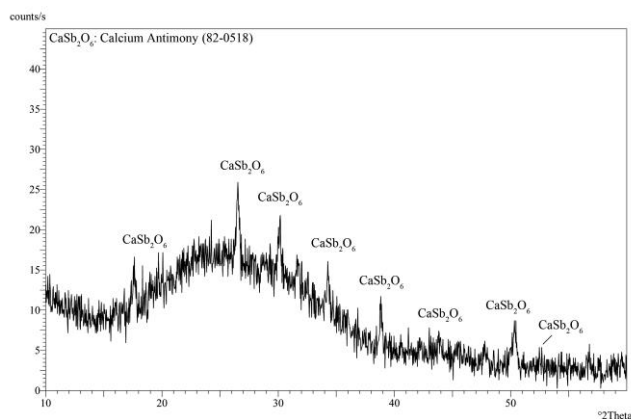
Figure 9. XRD pattern of light brown tesserae
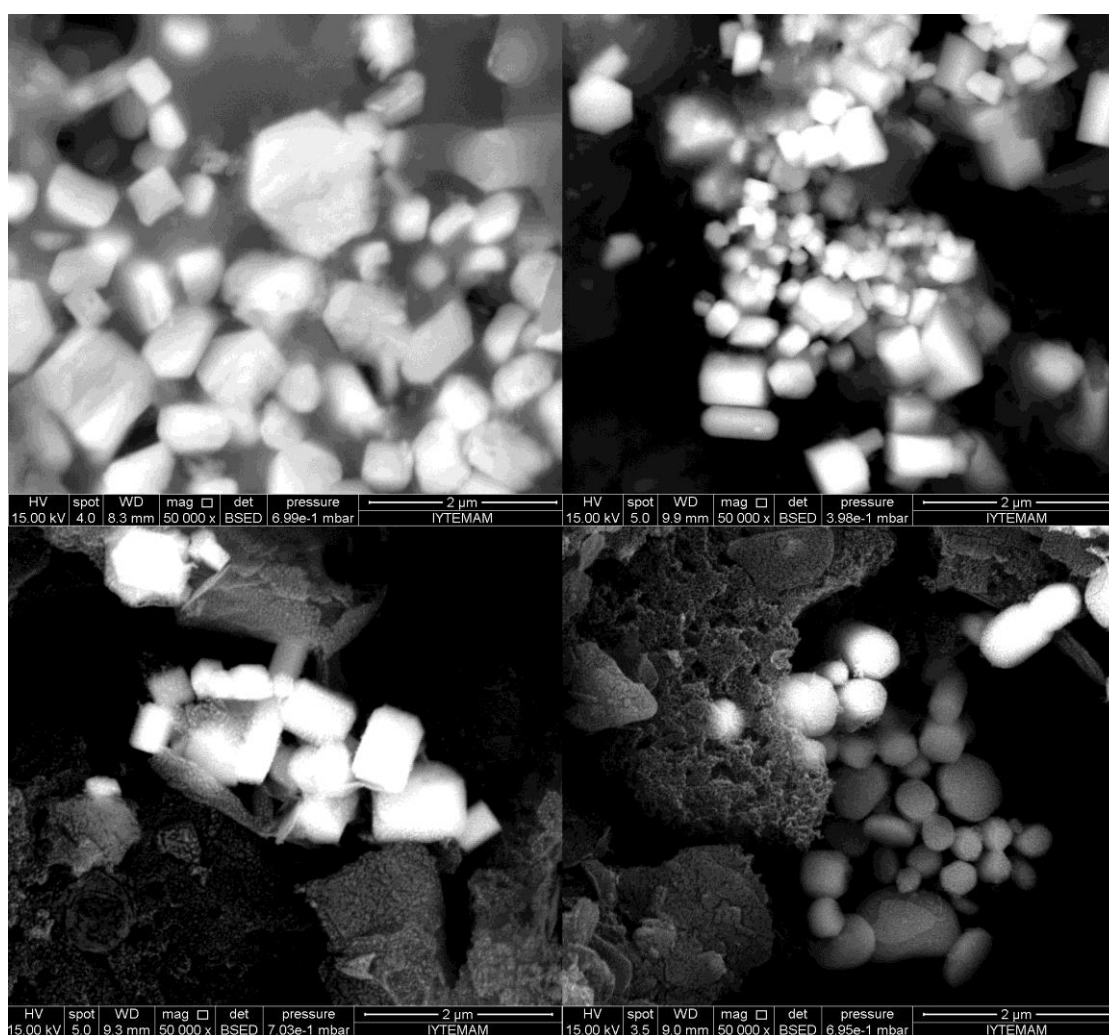
Figure 10. BSE images of Ca antimonate crystals as hexagonal in blue (a), cyan (b), dark turquoise (c), and turquoise (d).

Colorants of the glasses were determined by XRF analysis (Table 3). All analyzed tesserae were colored by transition metal compounds. The colorants are cobalt, copper, manganese and iron that are typical of the Roman Period (Henderson, 1991; Lahlil et al., 2010a, 2010b, 2008; Werf et al., 2009). They dis-

solve in the glass melt in varying oxidation states or precipitate as metals by redox reactions giving color to the glass (Möncke et al., 2014).

Green color of the Lg, Dg1, Dg2, G1 and G2 tesserae were obtained by adding $Pb_2Sb_2O_7$ (yellow) to the transparent blue glasses. Based on the theory of

color, the addition of yellow to blue modifies the color towards greenish hues, in opaque glass this effect can be obtained by introducing yellow crystals in a transparent blue glass. CuO (0.88-2.65 wt %) were also responsible for the greenish hues of the glasses with $Pb_2Sb_2O_7$ (Arletti et al., 2006a; Croveri et al., 2010). Therefore the variability of green tonality is certainly due to the abundance of copper oxide and contribution of bindheimite (yellow lead antimonite) crystals in varying amounts (Werf et al., 2009). The source of copper might be tin bronze due to the presence of tin oxide in the chemical composition of the green tesserae due to weight percent ratio of tin to copper as approximately 0.1 (Brill, 1988; Brun et al., 1991; Freestone, 1987; Gedzevičiute et al., 2009; Henderson, 1985; Werf et al., 2009).

As in green tesserae, yellow tesserae (Yt) contain higher PbO content, however contain lower amount of CuO than green tesserae. Higher amount of PbO in the form of lead antimonite, responsible for the yellow color, was detected in XRF, XRD analysis and SEM-BSE images. The use of lead antimonate crystals are noted as both opacifying and coloring agent for yellow and green tesserae in Roman and Byzantine Period (Croveri et al., 2010; Schibille et al., 2012; Werf et al., 2009).

White tessera contains Sb_2O_5 (1.68%) and low amounts of transition metal oxides, which are responsible for the intense colors. The Sb_2O_5 levels are lower than the other opaque glasses due to its semi opaque appearance. In recent studies, it has been indicated that white Roman and Byzantine glass tesserae were obtained using $CaSb_2O_6$ (~0.5%) (Schibille et al., 2012; Werf et al., 2009).

Turquoise and cyan tesserae (T1, T2, Dt, C1, C2) contain high amounts of CuO (3.25%, 0.74%, 2.56%, 0.35%, 0.30%) and lower CoO (nd, 0.02%, 0.003%, nd, 0.01%) respectively. In a soda lime silica glass, cobalt and copper ions both give blue color to the glass. Copper gives a greenish hue, whereas cobalt gives a deep blue color. Cobalt has higher absorption coefficient than the copper ions, therefore a few ppm of cobalt ions is enough to give bluish hue to the glass (Brill, 1999; Fiori and Macchiarola, 1998; Freestone and Bimson, 1995; Licenziati and Calligaro, 2015; Mirti et al., 2002; Nenna, 1999). The amount of copper and cobalt ions are directly related to the green and blue hue of the glass color. Different shades of turquoise and cyan can be obtained by introducing variable amounts of Ca-antimony that whiten and brighten up the color. This can be seen in the analyzed light turquoise tesserae (T1 and T2), that exhibit higher contents of Sb_2O_5 (3.46%, 3.44%) than the dark turquoise (Dt) (1.41%). Regarding the cyan tesserae (C1, C2), they exhibit higher amounts of Sb_2O_5 (4.07%, 4.22%) levels than the light turquoise sam-

ples. In turquoise and cyan tesserae, relative percentages of SnO_2 and CuO may be dependent on the use of a tin bronze as the copper source similar with yellow and green tesserae. In recent studies, the use of copper has been noted in Roman glasses to obtain blue-green colors (Arletti et al., 2011b; Croveri et al., 2010; Verita, 2000; Werf et al., 2009).

Blue tesserae (Lb, Bv-O, Bv-So) exhibit slightly higher cobalt levels (0.02%, 0.11%, 0.07%) responsible for the blue color of the glass. According to literature, cobalt is associated with copper, arsenic, iron or nickel, however any element related with the cobalt source was determined in the analysis (Arletti et al., 2006b; Fiori and Vandini, 2004; Henderson, 2000; Silvestri et al., 2012a). In addition, for the cobalt source an iron rich ore may have been used due to the higher iron levels of the blue glasses.

Dark red tessera contains high amounts of CuO (1.07%), Fe_2O_3 (3.81%), PbO (2.00%) and SnO_2 (0.1%). Iron and the copper ions are responsible for the red color of the glass. Iron is the most utilized colorant agent of the glass which is naturally found in the sand as an impurity. High iron content of the red glass suggests that it was intentionally added as a reducing agent for the copper (Brill, 1988). Copper gives bright red color of the glass as cuprite (CuO_2) which is a typical characteristic of the red glasses Freestone, 1987. Considerable amounts of tin indicates that copper was not added in the form of copper metal, it was added as bronze scale which dissolves easily (Brill and Cahill, 1988).

However, dark red tesserae contain much lower amounts of copper than ancient bright red colored tesserae also in the microstructural analysis there are no cuprite minerals. Consequently, it can be suggested that lower copper ions are responsible for the brownish red color and higher iron levels are responsible for the dark color of the Antandros dark red tesserae.

Black glass tesserae contain higher Fe_2O_3 (3.81%) and MnO (0.05%) and do not contain other transition metal oxides or Sb_2O_5. Ancient black glasses were produced by intentional addition of iron and manganese oxides to the glass batch without addition of other coloring agents (Henderson, 1985; Mass J. L et al., 2002). There were two types of black glasses with respect to their iron concentrations. If black glass contains low amounts of iron oxides (1-2% Fe_2O_3) this type of glass was produced in the Early Roman period, whereas if they contained high amounts of iron oxides (4-10% Fe_2O_3), they are produced after 150 AD. In addition, considering antimony concentrations of the glass, Levantine group glasses are contain antimony, however, Egyptian glasses do not contain antimony (Van Der Linden et al., 2009). Thus, black glass exhibits a different compositional charac-

teristic from other analyzed glass tesserae and may have been produced in a different period.

Light brown tesserae contain significant amounts of MnO (2.38%) and Sb_2O_5 (3.10%) which give the light brownish color to the glass. Manganese has been used as a colorant and a decolorizer and also as an oxidizer of iron ions which is balancing the greenish brown color of the raw glass (Fiori, 2015; Silvestri et al., 2012b; Vandini et al., 2006). Higher magnesium levels give an orange color to the glass (Möncke et al., 2014). Therefore, high amounts of Sb_2O_5 balance the orange color and provide a brownish color.

5. CONCLUSION

Antandros mosaic glass tesserae contradict historical Roman glass regarding the natron levels as fluxing agent which were traded from the Wadi Natrun in Egypt. Glasses were produced in a limited number of primary glass production centres with pure soda coming from the Wadi Natrun in Egypt and the sand was obtained locally. Later the produced glass batches were exported to secondary glass production centres where the glasses were turned into final products. In Roman Period, before the depletion of natron sources, glasses were produced with pure soda and contained higher amounts of natron. Although, Antandros glasses exhibited similar characteristics to Roman glasses, they have lower natron levels. This is supporting two production possibilities in the production of Antandros glasses. First, natron might have been provided from another or a new source due to the shortage of natron in Wadi Natrun. Second, glass manufacturers succeeded in producing glass with low flux addition due to economic reasons. Regarding the silica sources, in the production of Antandros tesserae, coastal sand was used from Palestine coast similar with Levantine I group glasses except for black tesserae.

Glasses were all opacified with antimony oxides and coloured with transition metal oxides. These are typical characteristics of Roman period except black tesserae which do not contain antimony oxides. The amount of the colorants and their abundance effects the hue and brightness of the glass. In addition, composition of the glass influences the effects of the colorants especially the amount of opacifiers influence the effect of the colorants. Furthermore, colorimetric coordinates of the glasses are in accordance with the chemical composition of the Antandros glasses. Antandros glasses were most probably produced in a nearby local production centre in Assos ancient city. Besides lower natron levels, all the analysed glasses were soda lime silica glasses that show similar compositions of Roman antimony-decoloured glasses except black one. Black tesserae exhibit a different production technology and raw materials. It may have been produced at a different production period. Analytical data of glass from Anatolia and potential silica sources in the region are insufficient thus more analytical studies need to be conducted.

REFERENCES

Ali, N., Abd-allah, R., 2015. the Authentication and Characterization of Glass Objects Excavated From Tell Es-Sukhnah , Jordan 15, 39–50.

Arinat, M., Shiyyab, A., Abd-Allah, R., 2014. Byzantine glass mosaics excavated from the "cross church", Jerash, Jordan: An archaeometrical investigation. Mediterr. Archaeol. Archaeom. 14, 43–53.

Arletti, R., Conte, S., Vandini, M., Fiori, C., Bracci, S., Bacci, M., Porcinai, S., 2011a. Florence Baptistery: Chemical and Mineralogical Investigation of Glass Mosaic Tesserae. J. Archaeol. Sci. 38, 79–88. doi:10.1016/j.jas.2010.08.012

Arletti, R., Dalconi, M.C., Quartieri, S., Triscari, M., Vezzalini, G., 2006a. Roman Coloured and Opaque Glass: a Chemical and Spectroscopic Study. Appl. Phys. A 83, 239–245. doi:10.1007/s00339-006-3515-2

Arletti, R., Quartieri, S., Vezzalini, G., 2006b. Glass mosaic tesserae from Pompeii: An archeometrical investigation. Period. di Mineral. 75, 25–38.

Arletti, R., Vezzalini, G., Fiori, C., Vandini, M., 2011b. Mosaic Glass From St Peter'S, Rome: Manufacturing Techniques and Raw Materials Employed in Late 16Th-Century Italian Opaque Glass. Archaeometry 53, 364–386. doi:10.1111/j.1475-4754.2010.00538.x

Bimson, M., Freestone, I.C., 1988. Some Egyptian Glasses Dated by Royal Inscription. J. Glass Stud. 30, 11–15.

Brill, R.H., 1999. Chemical Analyses of Early Glasses.

Brill, R.H., 1988. Scientific investigations of the Jalame glass and related finds. Excav. Jalame site a Glas. Fact. late Rom. Palest. 257–295.

Brill, R.H., 1968. The Scientific Investigation of Ancient Glasses.

Brill, R.H., Cahill, N.D., 1988. A Red Opaque Glass From Sardis and Some Thoughts on Red Opaques In General. J. Glass Stud. 30, 16–27.

Brun, N., Mazerolles, L., Pernot, M., 1991. Microstructure of Opaque Red Glass Containing Copper. J. Mater. Sci. Lett. 10, 1418–1420. doi:10.1007/BF00735696

Ceglia, A., Cosyns, P., Nys, K., Terryn, H., Thienpont, H., Meulebroeck, W., 2015. Late antique glass distribution and consumption in Cyprus: a chemical study. J. Archaeol. Sci. 61, 213–222. doi:10.1016/j.jas.2015.06.009

Costagliola, P., Baldi, G., Cipriani, C., 2000. Mineralogical and Chemical Characterisation of the Medicean Glass Mosaic Tesserae and Mortars of the Grotta del Buontalenti, Giardino di Boboli, Florence. J. Cult. Herit. 1, 287–299.

Croveri, P., Fragalà, I., Ciliberto, E., 2010. Analysis of Glass Tesserae from the Mosaics of the "Villa del Casale" near Piazza Armerina (Enna, Italy). Chemical Composition, State of Preservation and Production Technology. Appl. Phys. A 100, 927–935. doi:10.1007/s00339-010-5670-8

Fiori, C., 2015. Production technology of Byzantine red mosaic glasses. Ceram. Int. 41, 3152–3157. doi:10.1016/j.ceramint.2014.10.160

Fiori, C., Macchiarola, M., 1998. Studio e confronti fra la composizione chimica di vetri del II-I sec. A.C. Provenienti da delos (grecia) e vetri provenienti dalla capitanata (fg): Herdonia, I-II sec. D.c., arpi e ascoli satriano, II sec. A.c. Atti 2e Giornate Naz. di Stud. AIHV - Com. Naz. Ital. 139–146.

Fiori, C., Vandini, M., 2004. Chemical composition of glass and its raw materials: chronological and geographical development in the first millennium A. D., When Glass Matters. Studies in the History of Science and Art from Graeco-Roman Antiquity to Early Modern Era. Leo S. Olschki, Florence.

Fiori, C., Vandini, M., Mazzotti, V., 2003. Colore e Tecnologia Degli Smalti Musivi dei Riquadri di Giustiniano e Teodora Nella Basilica di San Vitale a Ravenna. Ceramurgia 33, 135–154.

Foy, D., 2000. Technologie, géographie, économie: les ateliers de verriers primaires et secondaires en Occident. Esquisse d'une évolution de l'Antiquité au Moyen Âge. La route du verre. Ateliers primaires Second. du Second millénaire avond J.C. au Moyen Age 147–170.

Freestone, I., 1987. Composition and Microstructure of Early Opaque Red Glass. Early Vitr. Mater. 56, 173–191.

Freestone, I.C., 2006. Glass production in Late Antiquity and the Early Islamic period: a geochemical perspective. Geomaterials Cult. Herit. 257, 201–216. doi:10.1144/GSL.SP.2006.257.01.16

Freestone, I.C., 2005. The provenance of ancient glass through compositional analysis. Mater. Res. Soc. Symp. Proc. 852, 1–14. doi:10.1557/PROC-852-OO8.1

Freestone, I.C., 2000. Nature [14, 17]. 1–17.

Freestone, I.C., Bimson, M., 1995. Early Venetian Enamelling on Glass: Technology and Origins. MRS Proc. doi:10.1557/PROC-352-415

Freestone, I.C., Gorin-Rosen, Y., 1999. The great glass slab at Bet She'arim, Israel: an early islamic glassmaking experiment. J. Glass Stud. 41, 105–116.

Freestone, I.C., Hughes, M.J., 2006. The origins of the Jarrow glass. Wearmouth Jarrow Monast. Sites Vol. 2 2, 147–155.

Freestone, I.C., Jackson-Tal, R.E., Taxel, I., Tal, O., 2015. Glass production at an Early Islamic workshop in Tel Aviv. J. Archaeol. Sci. 62, 45–54. doi:10.1016/j.jas.2015.07.003

Freestone, I.C., Leslie, K.A., Thirlwall, M., Gorin-Rosen, Y., 2003. Strontium Isotopes in the Investigation of Early Glass Production: Byzantine and Early Islamic Glass from the Near East. Archaeometry 45, 19–32.

Freestone, I.C., Ponting, M., Hughes, M.J., 2002. The origins of Byzantine glass from Maroni Petrera, Cyprus. Archaeometry 44, 257–272. doi:10.1111/1475-4754.t01-1-00058

Gedzevičiute, V., Welter, N., Schüssler, U., Weiss, C., 2009. Chemical composition and colouring agents of Roman mosaic and millefiori glass, studied by electron microprobe analysis and Raman microspectroscopy. Archaeol. Anthropol. Sci. 1, 15–29. doi:10.1007/s12520-009-0005-4

Gratuze, B., Barrandon, J.N., 1990. Islamic glass weights and stamps: analysis using nuclear techniques. Archaeometry 32, 155–162.

Henderson, J., 2000. The Science and Archaeology of Materials: An Investigation of Inorganic Materials.

Routledge, London.

Henderson, J., 1991. Chemical Characterization Of Roman Glass Vessels, Enamels And Tesserae In Vandiver. Mater. Issues Art Archaeol. 2, 601–720.

Henderson, J., 1988. Electron Probe Microanalysis of Mixed-Alkali Glasses. Archaeometry 30, 77–91.

Henderson, J., 1985. The Raw Materials of Early Glass Production. Oxford J. Archaeol. 4, 267–292. doi:10.1111/j.1468-0092.1985.tb00248.x

Jackson, C.M., Hunter, J.R., Warren, S.E., Cool, H.E.M., 1991. The analysis of blue-green glass and glassy waste from two Romano-British glass working sites. Archaeometry 90, 295–304.

Lahlil, S., Biron, I., Cotte, M., Susini, J., 2010a. New Insight on the in Situ Crystallization of Calcium Antimonate Opacified Glass During the Roman Period. Appl. Phys. A 100, 683–692. doi:10.1007/s00339-010-5650-z

Lahlil, S., Biron, I., Cotte, M., Susini, J., Menguy, N., 2010b. Synthesis of Calcium Antimonate Nano-Crystals by the 18th Dynasty Egyptian Glassmakers. Appl. Phys. A Mater. Sci. Process. 98, 1–8.

Lahlil, S., Biron, I., Galoisy, L., Morin, G., 2008. Rediscovering ancient glass technologies through the examination of opacifier crystals. Appl. Phys. A 92, 109–116. doi:10.1007/s00339-008-4456-8

Lauwers, V., Degryse, P., Waelkens, M., 2007. Evidence for Anatolian Glassworking in Antiquity: the Case of Sagalassos (Southwestern Turkey). J. Glass Stud.

Licenziati, F., Calligaro, T., 2015. Study of mosaic glass tesserae from Delos, Greece using a combination of portable μ-Raman and X-ray fluorescence spectrometry. J. Archaeol. Sci. Reports. doi:10.1016/j.jasrep.2015.10.017

Lilyquist, C., Brill, R., Wypsyski M. T, 1993. Studies in Ancient Egyptian Glass. The Metropolitan Museum of Art, New York.

Mass J. L, Wypsyski M. T, Stone R. E, 2002. Malkata and Lisht Glassmaking Technologies: Towards a Specific Link Between Second Millenium BC Metallurgists and Glassmakers. Archaeometry 1, 67–82.

Mirti, P., Davit, P., Gulmini, M., 2002. Colourants and Opacifiers in Seventh and Eighth Century Glass Investigated by Spectroscopic Techniques. Anal. Bioanal. Chem. Chem. 372, 221–229. doi:10.1007/s00216-001-1183-9

Möncke, D., Papageorgiou, M., Winterstein-Beckmann, A., Zacharias, N., 2014. Roman Glasses Coloured by Dissolved Transition Metal Ions: Redox-Reactions, Optical Spectroscopy and Ligand Field Theory. J. Archaeol. Sci. 46, 23–36. doi:10.1016/j.jas.2014.03.007

Nenna, M.D., 1999. Exploration archéologique de Délos Fascicule XXXVII Les verres. Ecole française d'Athènes diff. de Boccard, Athènes Paris.

Newton, R., Davison, S., 1989. Conservation of Glass. Butterworth Heinemann, Oxford.

Paynter, S., Kearns, T., Cool, H., Chenery, S., 2015. Roman coloured glass in the Western provinces: The glass cakes and tesserae from West Clacton in England. J. Archaeol. Sci. 62, 66–81. doi:10.1016/j.jas.2015.07.006

Polat, G., 2002. Antandros 2001 Yılı Kazıları, 24. Kazı Sonuçları Toplantısı, Cilt 2. Ankara.

Polat, G., Polat, Y., 2005. Antandros 2003-2004 Yılı Kazıları, 27. Kazı Sonuçları Toplantısı, Cilt 2,. Ankara.

Polat, G., Polat, Y., Yağız, K., 2007. Antandros 2005 Yılı Kazıları, 28. Kazı Sonuçları Toplantısı - II. Cilt. Ankara.

Quien M. Le, 1958. Oriens christianus 1. Graz.

Rehren, T., Connolly, P., Schibille, N., Schwarzer, H., 2015. Changes in glass consumption in Pergamon (Turkey) from Hellenistic to late Byzantine and Islamic times. J. Archaeol. Sci. 55, 266–279. doi:10.1016/j.jas.2014.12.025

Rehren, T., Freestone, I.C., 2015. Ancient glass: from kaleidoscope to crystal ball. J. Archaeol. Sci. 56, 233–241. doi:10.1016/j.jas.2015.02.021

Sayre E. V, Smith R. W, 1961. Compositional Categories of Ancient Glass. Am. Assoc. Adv. Sci. 133, 1824–1826.

Schibille, N., 2011. Late Byzantine mineral soda high alumina glasses from Asia Minor: a new primary glass production group. PLoS One 6, e18970. doi:10.1371/journal.pone.0018970

Schibille, N., Degryse, P., Corremans, M., Specht, C.G., 2012. Chemical Characterisation of Glass Mosaic Tesserae from Sixth-Century Sagalassos (south-west Turkey): Chronology and Production Techniques. J. Archaeol. Sci. 39, 1480–1492. doi:10.1016/j.jas.2012.01.020

Shortland, A.J., Tite, M.S., 2000. Raw Materials of Glass From Amarna and Implications for The Origins Of Egyptian Glass. Archaeometry 1, 141–151.

Silvestri, A., Molin, G., Salviulo, G., 2008. The colourless glass of Iulia Felix. J. Archaeol. Sci. 35, 331–341. doi:10.1016/j.jas.2007.03.010

Silvestri, A., Tonietto, S., D'Acapito, F., Molin, G., 2012a. The Role of Copper on Colour of Palaeo-Christian Glass Mosaic Tesserae: An XAS study. J. Cult. Herit. 13, 137–144. doi:10.1016/j.culher.2011.08.002

Silvestri, A., Tonietto, S., Molin, G., 2011. The palaeo-Christian glass mosaic of St. Prosdocimus (Padova, Italy): archaeometric characterisation of "gold" tesserae. J. Archaeol. Sci. 38, 3402–3414. doi:10.1016/j.jas.2011.07.027

Silvestri, A., Tonietto, S., Molin, G., Guerriero, P., 2012b. The Palaeo-Christian Glass Mosaic of St. Prosdocimus (Padova, Italy): Archaeometric Characterisation of Tesserae with Antimony- or Phosphorus-Based Opacifiers. J. Archaeol. Sci. 39, 2177–2190. doi:10.1016/j.jas.2012.03.012

Smith J.T, 1997. Roman Villas. A Study in Social Structure, London and New York: Routledge. doi:10.1017/CBO9781107415324.004

Strabo, 2000. Geographika, Arkeoloji Sanat Yayınları. İstanbul. doi:10.1017/CBO9781107415324.004

Tite, M., Pradell, T., Shortland, A.J., 2007. Discovery, Production and Use of Tin-Based Opacifiers in Glasses, Enamels and Glazes From the Late Iron Age Onwards: a Reassessment. Archaeometry 0, 071024000902001–??? doi:10.1111/j.1475-4754.2007.00339.x

Turner, W.E.S., 1956. Studies in Ancient Glasses and Glassmaking Processes: Raw Materials and Melting Processes. part V.

Uhlir, K., Melcher, M., Czurda-Ruth, B., Schreiner, M., Krinzinger, F., 2006. Scientific investigations on ancient glasses from Hanghaus I in Ephesos/Turkey using SEM/EDX and μ-XRF. Proc. 36th Int. Symp. Archaeom. May 2nd - 6th, 2006, Quebec City, Canada 6–11.

Van Der Linden, V., Cosyns, P., Schalm, O., Cagno, S., Nys, K., Janssens, K., Nowak, A., Wagner, B., Bulska, E., 2009. Deeply coloured and black glass in the northern provinces of the Roman empire: Differences and similarities in chemical composition before and after AD 150. Archaeometry 51, 822–844. doi:10.1111/j.1475-4754.2008.00434.x

Vandini, M., Fiori, C., Cametti, R., 2006. Classification and Technology of Byzantine Mosaic Glass. Ann. Chim. 96, 587–599.

Verita, M., 2000. Technology and Deterioration of Vitreous Mosaic Tesserae. Rev. Conserv. 1, 65–76.

Wedepohl, K.H., Baumann, A., 2000. The use of marine molluskan shells for Roman glass and local raw glass production in the Eifel area (Western Germany). Naturwissenschaften 87, 129–132.

Werf, I., Mangone, A., Giannossa, L.C., Traini, A., Laviano, R., Coralini, A., Sabbatini, L., 2009. Archaeometric Investigation of Roman Tesserae from Herculaneum (Italy) by the Combined Use of Complementary Micro-Destructive Analytical Techniques. J. Archaeol. Sci. 36, 2625–2634. doi:10.1016/j.jas.2009.07.015

Yalman, B., 1993. Antandros Nekropolisi Kurtarma Kazısı, III. Müze Kurtarma Kazlar Semineri. Ankara.